European Journal of Cell Biology 101 (2022) 151282

Contents lists available at ScienceDirect

European Journal of Cell Biology

journal homepage: www.elsevier.com/locate/ejcb

Short communication

Paneth cells drive intestinal stem cell competition and clonality in aging and calorie restriction

Francesco Annunziata, Seyed Mohammad Mahdi Rasa, Anna Krepelova, Jing Lu, Alberto Minetti, Omid Omrani, Suneetha Nunna, Lisa Adam, Sandra Käppel, Francesco Neri *

Leibniz Institute on Aging – Fritz Lipmann Institute (FLI), Jena, Germany

ARTICLE INFO

Keywords:
Intestinal stem cells
Clonal drift
Aging
Calorie restriction
Niche paneth cells

ABSTRACT

Calorie restriction has been recently shown to increase intestinal stem cell competition and to reduce mutation fixation in young mice. However, the impact of aging on this process is unknown. By employing Confetti reporter mice, here we show that, unexpectedly, old mice have more intestinal stem cell (ISC) competition than young mice. Moreover, differently from what observed in young mice, calorie restriction, when applied at late-life, decreases this process. Importantly, we also observed a strong correlation between the ISC competition and Paneth cell number. *In vivo* analysis and *in vitro* organoid experiments indicated that Paneth cells play a major role in driving intestinal stem cell competition and crypt clonality. Taken together, our results provide evidence that increasing the number of Paneth cells can increase the number of competitive ISCs, representing a valuable therapeutic target to delay fixation of mutated intestinal stem cells.

1. Introduction

The small intestine is composed by finger-like structures called villi and U-shape structures called crypts of Lieberkuhn, in which reside intestinal stem cells (ISCs). ISCs are tightly in contact with fully differentiated secretory Paneth cells (PCs), the main source of crypt niche factors such as EGF, TGF-a, and Notch ligand Dll4 necessary for ISCs maintenance (van der Flier and Clevers, 2009; Sato et al., 2010). ISCs specifically express the Lgr5 gene (Barker et al., 2009). Lineage tracing experiments show that Lgr5 stem cells compete with neighboring ISCs for space and niche factors within a crypt. The result of this competition is that all cells that compose one crypt will derive from a single ISC that became "dominant" and replaced all other ISCs within said crypt (Winton and Ponder, 1990; Snippert et al., 2010; Lopez-Garcia, 2010).

Aging is a complex multifactorial biological process shared by all living vertebrates. A prominent aging feature is the decline in homeostatic and regenerative potential of stem cells and their surrounding niches (Oh et al., 2014). In intestine, sorted Lgr5 cells from old mice showed reduced efficiency in organoid formation when compared to the young Lgr5 cells (Pentinmikko et al., 2019; Uchida et al., 2019). ISCs depend on the balance between cell proliferation and differentiation to maintain a healthy intestinal epithelium. The homeostasis of this process is regulated by Wnt/beta-catenin signaling (Janeckova et al., 2016; Kabiri et al., 2018; Cui et al., 2019). It has been demonstrated that a reduction in Wnt signaling leads to a reduction in the number of wild-type (WT) ISCs that can compete with mutated (APC-deficient) ISCs, leading to a faster fixation of mutant ISCs within a crypt (Huels et al., 2018). Calorie Restriction (CR), a reduction of 20–40% in the daily calorie intake without any malnutrition, has been demonstrated to have beneficial effects in many tissues in a wide range of organisms (Colman et al., 2009; Fontana, Partridge and Longo, 2010). In young mouse intestine, CR has been demonstrated to increase the number and functionality of ISCs (Yilmaz et al., 2012; Igarashi et al., 2016; Bruens et al., 2020) and therefore to increase the number of WT ISCs that can compete and replace mutated ISCs (Bruens et al., 2020). However, the benefits of CR in aged organisms are largely controversial and its effects on aged ISC competition are completely unknown. Here, to address how ISC competition is affected during aging and upon CR diet, we employed the inducible Cre-reporter multicolor Confetti system that by random activation of one of the fluorescent markers in each cell upon recombinase reaction, allows to distinguish cells arising from different ISCs.

* Corresponding author.
E-mail addresses: francesco.neri@unito.it, francesco.neri@leibniz-fli.de (F. Neri).

https://doi.org/10.1016/j.ejcb.2022.151282
Received 12 July 2022; Received in revised form 3 November 2022; Accepted 3 November 2022
Available online 4 November 2022

2. Results

2.1. Aging increases intestinal stem cell competition

To investigate the impact of aging on ISC competition, we performed lineage tracing experiments by employing young and old mice carrying a Cre-reporter multicolor Confetti system (Rosa26-lsl-Confetti;Villin-creERT^2). Young (8–12 weeks old) and old (80–85 weeks old) Rosa26-lsl-Confetti;Villin-creERT^2 were intraperitoneally injected with 5 doses of tamoxifen (each dose of 100 mg/Kg of body weight) for 5 subsequent days (Fig. 1a). Following tamoxifen injections, all intestinal epithelial cells, including the ISCs, were labelled with one of the fluorescent proteins from the Confetti construct: green fluorescent protein (GFP), red fluorescent protein (RFP), cyan fluorescent protein (CFP), and yellow fluorescent protein (YFP). However, as already reported, the GFP frequency of recombination was lower than 1% and therefore excluded from the subsequent analyses (Snippert et al., 2010). In all figures the YFP was represented with the color green instead of yellow. At Time

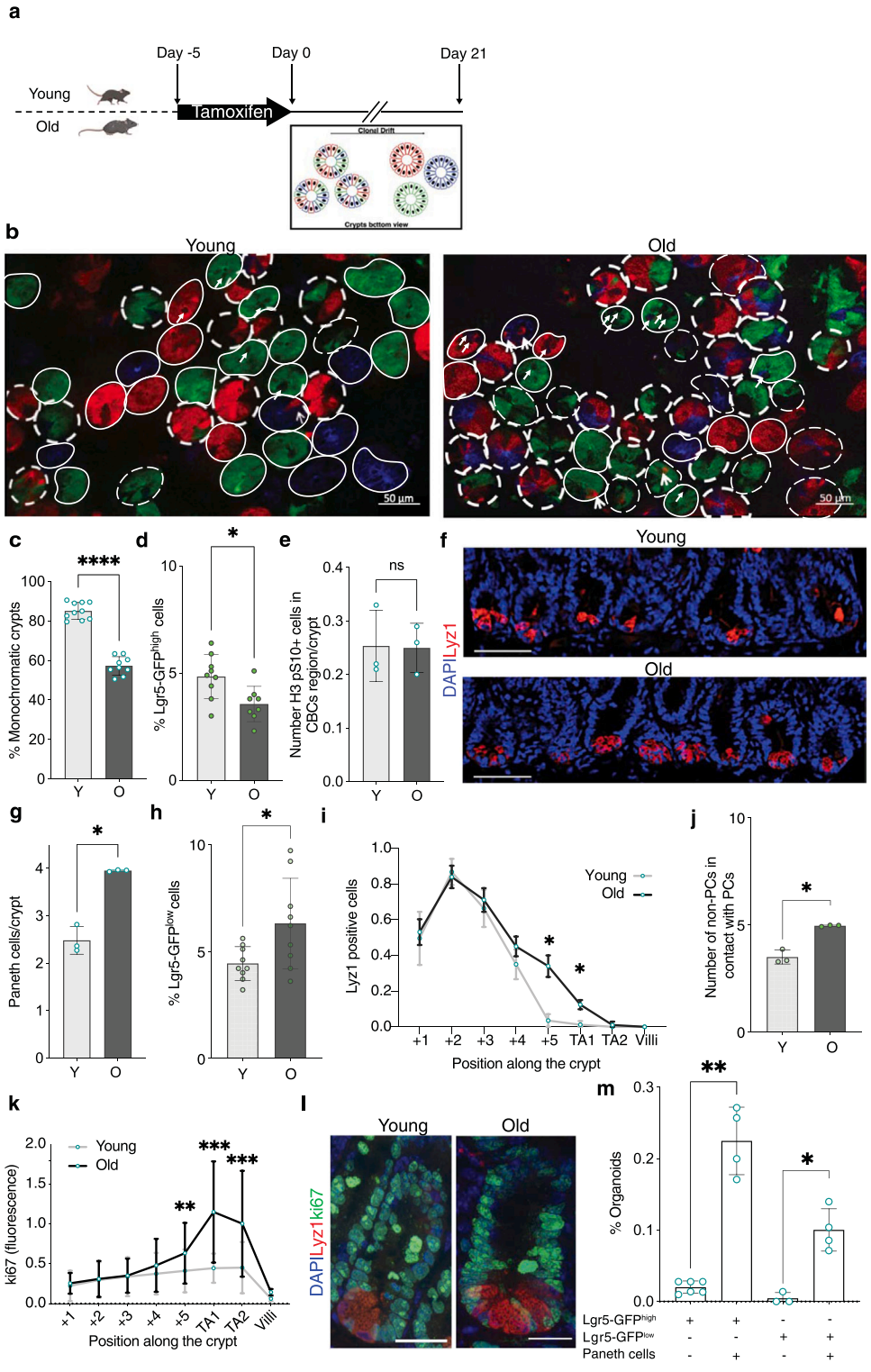

Fig. 1. Aging increases intestinal stem cell competition. a, Scheme of the experimental setting for lineage tracing experiment in young (8–12 weeks old) and old (80–85 weeks old) Rosa26-lsl-Confetti;Villin-creERT^2 mice. b, Representative images of intestinal sections from young and old mouse intestine 21 days post last tamoxifen injection. White circles represent monochromatic crypts. White dashed circles represent heterochromatic crypts. White arrows indicate Paneth cells. Scale bar 50 µm. c, Monochromatic crypts quantification from young and old mouse intestine. Young n = 10; Old n = 9. The number of crypts scored for each animal is ≥ 200. d, Fluorescence-activated cell sorting analysis (FACS) quantification of Lgr5-GFP^{high} cells in crypts from young (8–12 weeks old) and old (80–90 weeks old) Lgr5-EGFP-IRES-creERT^2 mice. Young n = 9; Old n = 9. e, Quantification of the H3-pS10 positive cells in each Crypt Base Columnar (CBC) cells region in the intestine of young and old mice. Young n = 3; Old n = 3. f, Representative images of Lyz1 immunofluorescence on young and old mouse intestine. Scale Bar 50 µm. Young n = 3; Old n = 3. The number of crypts scored is ≥ 45. g, Lyz1 immunofluorescence quantification from young and old mouse intestine. Young n = 3; Old n = 3. h, Fluorescence-activated cell sorting analysis (FACS) quantification of Lgr5-GFP^{low} cells in crypts from young and old Lgr5-EGFP-IRES-creERT^2 mice. Young n = 9; Old n = 9. i, Quantification of Lyz1 + cells / crypt in according to the cell position of the small intestinal crypts. The cell residing at the center of the bottom of the crypt is the number 1. TA1 represents the lower part of the Transit-Amplifier cells region (position ~6–8), while TA2 the upper part (positions ~9–11). Quantification on at least three different mice n = 3 and > 15 crypts analyzed for each mouse). j, Quantification of the non-Paneth cells in contact with PCs along the crypt. Young n = 3; Old n = 3. k, Quantification of the ki67 immunofluorescence signal (normalized on DAPI) for each cell residing at a different position of the small intestinal crypts as in Fig. 1i. l, Representative images of Lyz1 and ki67 immunofluorescence on young and old mouse intestine. Scale Bar 20 µm. m, Bar chart indicating the organoid-forming efficiency (in percentage) of the indicated conditions. n ≥ 3. Quantification represents mean ± SD. Dots represent individual animals. Shapiro Wilk test was used to calculate the normality. Significance was determined by unpaired two-tail t-test with Welch's correction. * p-Value ≤ 0.05, ** p-Value ≤ 0.01, *** p-Value ≤ 0.001, **** p-Value ≤ 0.0001, ns p-Value > 0.05.

0 (T0), no significant differences were observed in recombination and labelling efficiency of intestinal crypts from young and aged mice (Fig. S1a,b). At 21 days post tamoxifen injection, we observed a lower number of monochromatic crypts in old mice compared to the young mice, presumably reflecting an increase in ISC competition (Fig. 1b,c). It has been shown that the ISC competition and crypt clonality in the intestine positively correlate with the number and the proliferative status of the ISCs (Vermeulen. et al., 2013). However, both of these two factors have been shown to be reduced in aging (Nalapareddy et al., 2017; Mihaylova et al., 2018; Pentinmikko et al., 2019). Accordingly, FACS analysis revealed that the number of the ISCs (Lgr5-GFP^{high}) (Barker et al., 2009) decreased with aging (Fig. 1d and Fig. S1c). Interestingly, we did not observe any difference in the number of ISCs (Crypt Base Columnar (CBC) cells) positive for H3pS10 (mitosis marker) between young and old mice (Fig. 1e). On the same line, we also did not observe any difference in the number of CBCs ki67 (proliferation marker) positive cells between young and old (Fig. S1d). These analyses indicated that these two factors are not involved in the increased ISC competition observed in old mice.

As previously reported, we observed a higher number of Paneth cells in intestinal crypts from old mice (PCs - marked by Lyz1 staining) (Nalapareddy et al., 2017) (Fig. 1f,g). Lgr5-GFP^{medium} and Lgr5-GFP^{low} cells are located just above the bottom of the crypts and in the initial part of the region containing Transit-Amplifying (TA) cells. Interestingly, we observed an increase of Lgr5-GFP^{low} cells in crypts from old mice (Fig. 1h), while Lgr5-GFP^{medium} cells did not show any significant change (Fig. S1e). To better characterize the increase of PCs in aged intestinal crypts and their potential connection with the ISC competition, we quantified the PCs distribution along the bottom-top axis of the intestinal crypts in young and old mice. We considered position + 1 the cell in the center of the base of the U-shaped crypt (Fig. 1i). Old mice showed an increase of PCs (and, as consequence, an increase of non-Paneth cells (non-PCs) in contact with a PC) in position + 5 and in the TA region close to the crypt base, where Lgr5-GFP^{low} cells reside (Fig. 1i,j). Remarkably, these two regions showed an increase of ki67 signal in non-PCs (Fig. 1k,l) indicating that these non-PCs (mostly Lgr5-GFP^{low} cells) may be in physical contact with PCs and triggered to proliferate. As already reported (Sato et al., 2010), we observed that plating Lgr5-GFP cells together with PCs in a 1:1 ratio increased the organoid-forming efficiency (Fig. S1f). However, when the Lgr5-PCs were purified as doublet and the reciprocal interaction maintained in culture, the organoid forming efficiency was significantly higher than plating them together after separated FACS purification (Fig. S1f). To demonstrate whether the PCs could also provide the Lgr5-GFP^{low} cells with a higher proliferative activity, we employed an *in vitro* regeneration assay by plating either Lgr5-GFP^{low} cells alone or in combination with PCs and testing their ability to form intestinal organoids. As control we plated Lgr5-GFP^{high} cells alone or in combination with PCs. Interestingly, the Lgr5-GFP^{low} cells co-cultured together with PCs increased the organoid-forming efficiency with respect to the Lgr5-GFP^{low} alone (Fig. 1m). These data strongly suggest that PCs can increase stemness and regeneration ability of all the Lgr5 positive cells, including the Lgr5-GFP^{low}, by physically get in touch with them.

2.2. Paneth cell number influences ISCs competition

Intestinal organoids are crypt-villus structures, composed of a central lumen and several crypt-like structures that contain ISCs and PCs (Sato et al., 2009). The advantage of using intestinal organoids is that the number of ISCs or PCs can be modulated by employing different growth media (Farin et al., 2012; Yin et al., 2013). Therefore, to investigate the functional correlation between ISC competition and the number of PCs, we generated organoids from intestinal crypts of Rosa26-lsl-Confetti; Villin-creERT^2 mice. Freshly isolated crypts were embedded in matrigel and seeded in the plate to grow as organoids (Sato et al., 2009). The crypts were immediately treated with 5 μM 4-hydroxytamoxifen (4-OHT) for 20 h to induce the recombinase reaction (Fig. S2a). At 3 days after 4-OHT induction each crypt-like structure was fully heterochromatic, while at day 13 more than 80% of the crypt-like structures became fully monochromatic (Fig. S2b,c), indicating that a crypt-like structure originated from a single ISC. We then applied the same experimental set up for intestinal crypts deriving from both young (8–12 weeks old) and old (80–85 weeks old) Rosa26-lsl-Confetti;Villin--creERT^2 mice (Fig. 2a). In contrast to what observed from *in vivo* experiments, old-mouse-derived organoids showed a higher number of monochromatic crypt-like structures than young-mouse-derived organoids (Fig. 2b,c), reflecting a lower degree of ISC competition. After 14 days of culturing, organoids maintained their young/old ISC ratio (Fig. 2d, quantification of cells expressing Olfm4, marker of ISCs (Yilmaz et al., 2012; Huels et al., 2018)) but organoids derived from old mice showed a significant reduction in the number of PCs with respect to young-mouse-derived organoids (Fig. 2e,f). This suggested that the number of PCs in old animals is modulated by crypt-extrinsic factors that are lost upon culturing *in vitro*. Moreover, these data further suggested that the number of PCs may represent a key factor in driving ISC competition and clonality capacity as well as could be responsible of the phenotype observed in old *in vivo*. To demonstrate it, we modulated the number of ISCs and PCs *in vitro* by employing different culturing media. Crypts from Rosa26-lsl-Confetti;Villin-creERT^2 mice were treated with 4-OHT to induce the recombinase reaction and cultured in 3 different conditions (Fig. 2g): 1) in standard ENR media (EGF, Noggin and R-Spondin-1), 2) in ENR media plus CHIR99021 (ENRC), which increases the number of ISCs as well the number of PCs (Yin et al., 2013) and 3) in ENR media plus CHIR99021 and valproic acid (ENRCV), which strongly increases the ISC number but decreases the PC number (Yin et al., 2013). To confirm the change in the number of ISCs and PCs following cell culture of the intestinal crypts in the 3 different culture media, we also treated crypts from Lgr5-EGFP-IRES-creERT^2 mice. Lgr5 (identified by GFP labelling) and Lyz1 co-staining confirmed the change in the number of ISCs and PCs (Fig. S2d-f). In Rosa26-lsl-Confetti;Villin-creERT^2 organoids, at 12 days after 4-OHT induction, we observed a lower number of crypt like structures when treated with CHIR99021 alone (ENRC). Conversely, valproic acid (ENRCV) fully rescued this phenotype (Fig. 2h,i). Altogether, these data indicate that the presence (and the amount) of PCs is a key factor in driving the ISC competition and crypt clonality even more than the absolute number or the proliferation rate of the ISCs.

2.3. Calorie restriction decreases ISC competition in old mice

In young mice, CR has been recently shown to increase ISC competition and reducing mutation fixation (Bruens et al., 2020). We therefore studied the CR effect in old mice by investigating whether CR could also modulate the number of PCs, thus representing a non-invasive approach to *in vivo* study the impact of the PCs on ISC clonal dominance. We used young (8–12 weeks old) (used as control experiment) and old (80–85 weeks old) Rosa26-lsl- Confetti;Villin-creERT^2 mice and kept them in *ad libitum* (AL) or CR diet. The mice were on CR for 39 days. From the fourteenth day to the eighteenth day of CR, in parallel with the CR feeding, young and old Confetti;Villin-creERT^2 mice were injected with 5 doses of tamoxifen (100 mg/Kg of body weight). The CR was continued for other 21 days, after which the mice were sacrificed for analysis (Fig. S3a).

Oppositely to young mice, in which CR increased ISC competition leading to a reduction of the monochromatic crypts, CR in old mice led to an increase of monochromatic crypts, indicating a reduction in ISC competition for crypt clonality (Fig. 3a,b and Fig. S3b). In young mice CR led to a slight significant increase in the number of ISCs, in old the number of ISCs also increased, but not significantly (Fig. S3c and Fig. 3c, d). In young mice, upon CR, we observed a general increase in cell proliferation rate all along the crypt axis (Fig. 3e-g and Fig. S3d). In old mice CR increased the ISC proliferation rate (Fig. 3f and Fig S3d), but

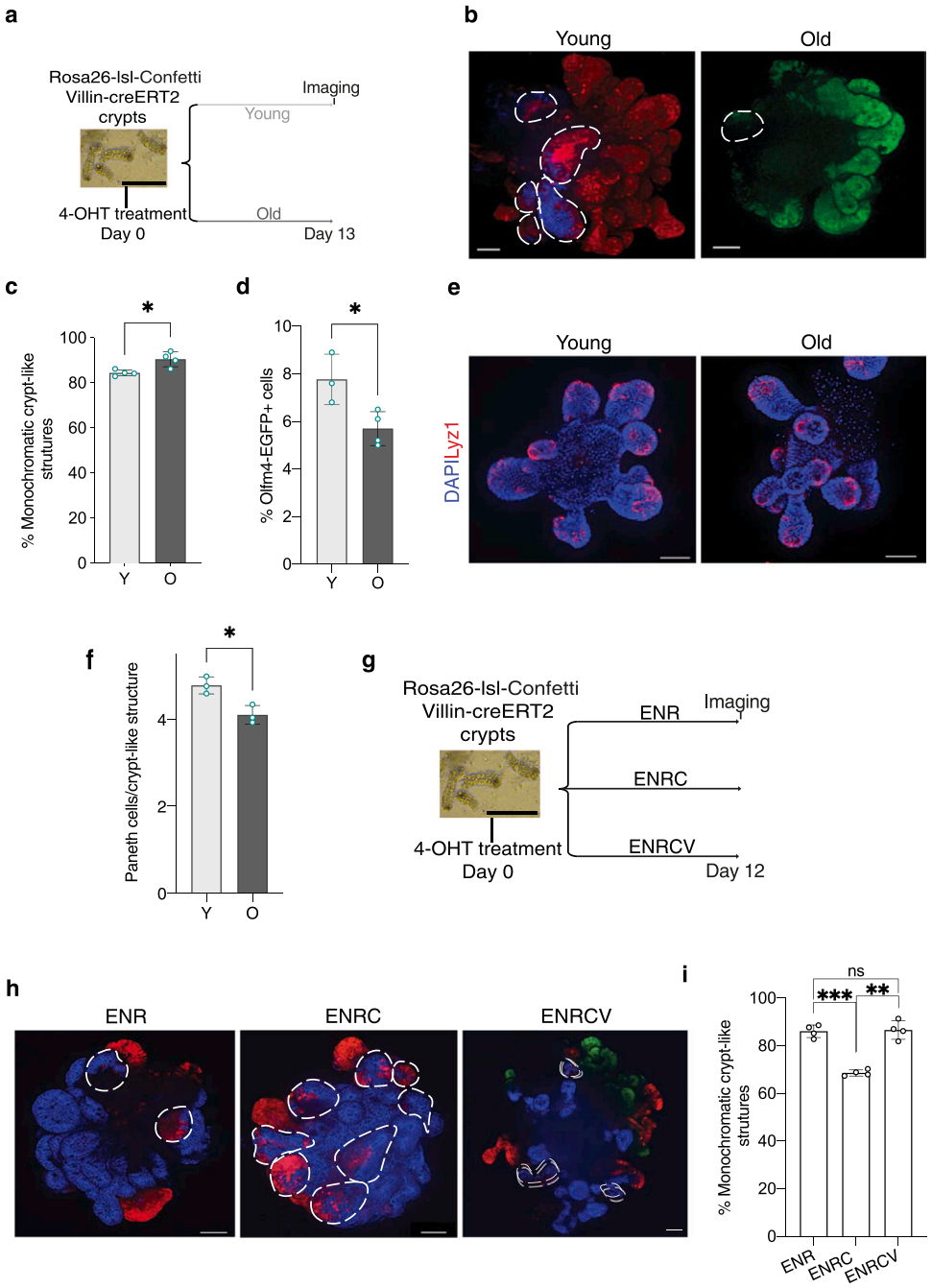

Fig. 2. Paneth cell number influence ISCs competition. a, Scheme of the experimental setting for lineage tracing experiment in Rosa26-lsl-Confetti;Villin-creERT^2 mouse organoids. b, Representative images of a young (8–12 weeks old) and old (80–85 weeks old) Rosa26-lsl-Confetti;Villin-creERT^2 derived organoid 13 days post 4-OHT. White dashed circles represent heterochromatic crypt-like structures. Scale Bar 100 μm. c, Quantification monochromatic crypt-like structures from young and old. Young n = 4; Old n = 4. For each animal ≥ 5 organoids were used for the quantification. d, FACS quantification of Olfm4-EGFP cells in organoids from young (8–12 weeks old) and old (80–90 weeks old) Olfm4-EGFP-IRES-creERT^2 mice kept in culture for 14 days. Young n = 4; Old n = 3. e, Representative images of Lyz1 immunofluorescence on young and old organoid kept in culture for 14 days. f, Quantification of Lyz1 positive cells per each crypt-like structure. Young n = 3; Old n = 3. For each animal ≥ 5 organoids were used for the quantification. g, Scheme of the experimental setting for lineage tracing experiment in Rosa26-lsl-Confetti;Villin-creERT^2 mouse organoids. h, Representative images of organoids 12 days post 4-OHT induction kept either in standard ENR media (left) either ENR media plus CHIR99021 (ENRC) (middle) or in ENR media plus CHIR99021 and valproic acid, with relative quantification. White dashed circles represent heterochromatic crypt-like structures. Scale bar 100 μm. i, Quantification monochromatic crypt-like structures. n = 4. For each animal ≥ 5 organoids were used for the quantification. Quantification represents mean ± SD. Dots represent individual animals. Shapiro Wilk test was used to calculate the normality. Significance was determined by unpaired two-tail t-test with Welch's correction. * p-Value ≤ 0.05, ** p-Value ≤ 0.01, *** p-Value ≤ 0.001, **** p-Value ≤ 0.0001, ns p-Value > 0.05.

oppositely from young mice, lead to a reduction in the number of H3pS10 +cells in the region above the ISC compartment (Fig. 3f,g). Importantly, and contrariwise to what observed in young mice, CR in old mice led to a reduction of the number of PCs in the intestinal crypts (Fig. 4a,b and Fig. S3e) indicating that the number of PCs (more than the ISC number) strongly influence the ISC competition. These data indicate that CR has opposite crypt-clonality effect in old compared to young mice and that, both in young and in old mice, PC number shows inverse correlation with the number of monochromatic crypts upon CR (Fig. 4c, d).

Taken together, our data showed the number of PCs is a key factor in regulating ISC competition and the process of crypt clonality. Restoring the number and the functionality of the PCs, possibly through non-invasive approaches like diet changes, may represent one the most promising medical therapy for many of the intestinal diseases, including colon cancer.

3. Discussion

Our data indicates that the number of ISCs and their proliferation rate are not the only parameters to take in consideration in the crypt clonality process, strongly supporting that the number of PCs may influence this process to an even greater extent. One scenario explaining the higher ISC competition observed in aged crypts is that in old mice the precursor cells (Lgr5-GFPlow cells), being physically in contact with PCs, may acquire higher clonogenicity potential and thus more frequently participating in the competition process and crypt colonization. Recently Azkanaz and colleagues showed that ISCs positioned away from the crypt base can function as long-term effective ISCs owing to a Wnt-dependent retrograde cellular movement, whilst the lack of

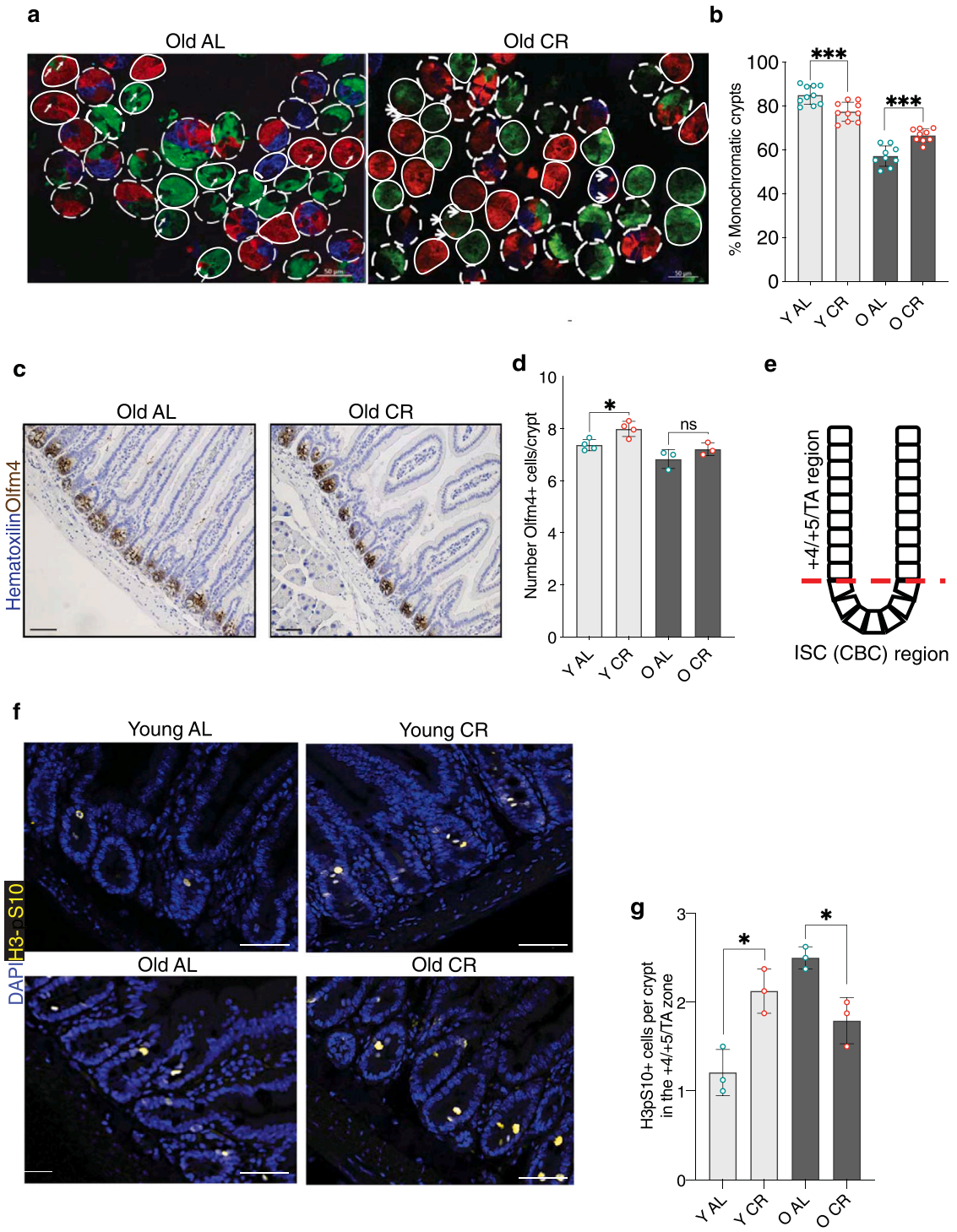

Fig. 3. Calorie restriction decreases intestinal stem cell competition in old mice. a, Representative images monochromatic crypts from old (80–85 weeks old) AL and old (80–85 weeks old) CR mouse intestine. White circles represent monochromatic chromatic crypts. White dashed circles represent heterochromatic crypts. White arrows indicate Paneth cells. Scale bar 50 μm. b, Monochromatic crypts quantification from young and old mouse intestine upon CR. Young AL n = 10; Young CR n = 10; Old AL n = 9; Old CR n = 9. The number of crypts scored for each animal is ≥ 200. c, Representative images of Olfm4 (intestinal stem cell marker) immunohistochemistry from old AL and CR mouse intestine. Scale bar 50 μm. d, Olfm4 immunohistochemistry quantification from young and old AL and CR mouse intestine. Young AL n = 4; Young CR n = 4; Old AL n = 4; Old CR n = 4. e, Schematic representation of crypt division used for quantification of H3-pS10 + cells along the crypt. f, Representative images of H3-pS10 immunofluorescence from young and old AL and CR mouse intestine. Scale bar 50 μm. g, H3-pS10 immunofluorescence quantification from young and old AL and CR + 4/+ 5/TA compartment. Young AL n = 3; Young CR n = 3; Old AL n = 3; Old CR n = 3. Quantification represents mean ± SD. Dots represent individual animals. Shapiro Wilk test was used to calculate the normality. Significance was determined by unpaired two-tail t-test with Welch's correction. * p-Value ≤ 0.05, ** p-Value ≤ 0.01, *** p-Value ≤ 0.001, **** p-Value ≤ 0.0001, ns p-Value > 0.05.

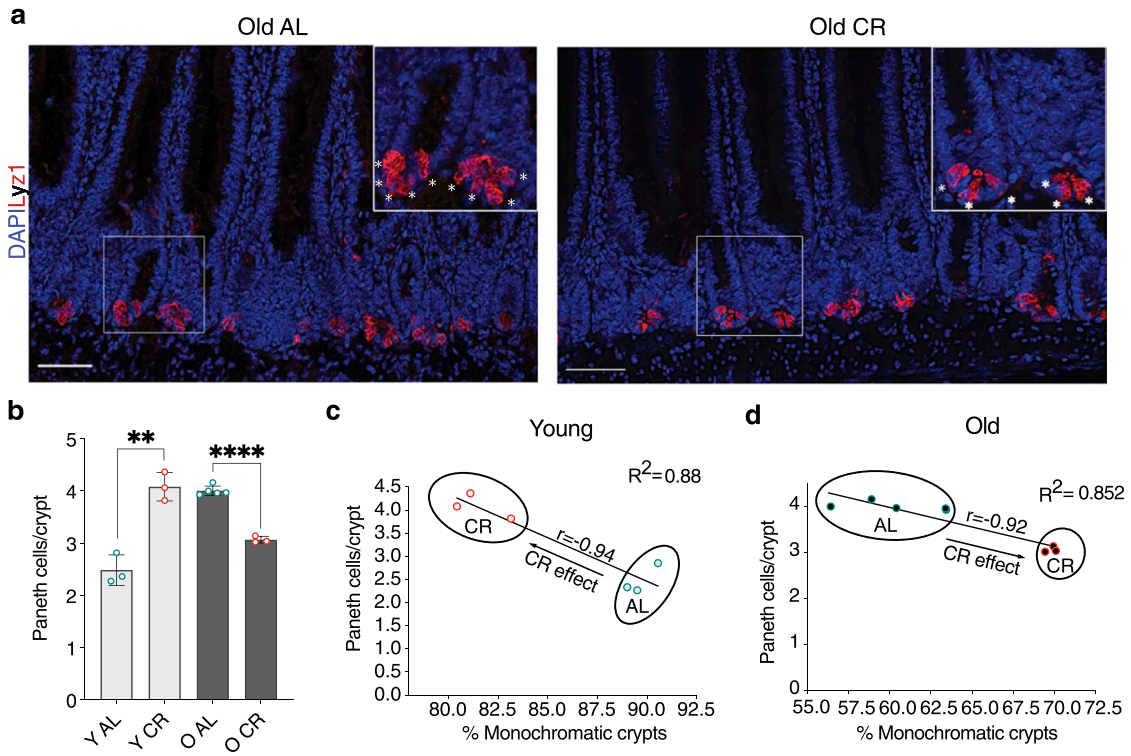

Fig. 4. Paneth cell analysis in the intestine of mice under calorie restriction. a, Representative images of Lyz1 immunofluorescence from old AL and old CR mouse intestine. Scale bar 50 μm. Asterisks indicate Paneth cells. The number of crypts scored is ≥ 45. b, Lyz1 immunofluorescence quantification from young and old AL and CR mouse intestine. Young AL n = 3; Young CR n = 3; Old AL n = 5; Old CR n = 3. c, Correlation analysis between monochromatic crypts and Paneth cell number per crypt in young AL and CR mice. Young AL n = 3; Young CR n = 3. d, Correlation analysis between monochromatic crypts and Paneth cell number per crypt in old AL and CR mice. Old AL n = 5; Old CR n = 3. Quantification represents mean ± SD. Dots represent individual animals. Shapiro Wilk test was used to calculate the normality. Significance was determined by unpaired two-tail t-test with Welch's correction. * p-Value ≤ 0.05, ** p-Value ≤ 0.01, *** p-Value ≤ 0.001, **** p-Value ≤ 0.0001, ns p-Value > 0.05.

retrograde movement leads to a reduction of effective ISCs (Azkanaz et al., 2022). In line with this observation, our study shows that fewer PCs, which are a source of Wnt signaling for ISCs, lead to fewer competitive ISCs, resulting in a faster clonal fixation. Conversely, a higher number of PCs could trigger a greater retrograde movement and make the Lgr5-GFPlow cells more effective and competitive leading to a slower clonal fixation.

A confirm that the number of PCs represents a key player in driving ISC competition and could be responsible of the phenotype observed in old mice, derives from our *in vitro* experiment. We observed that, oppositely to the *in vivo* analysis, old-mouse-derived organoids showed a lower ISC competition than young-mouse-derived organoids. The difference in the number of ISCs between young and old organoids kept in culture were still maintained, but organoids derived from old mice showed a reduction in the number of PCs with respect to those derived from young mice. To further demonstrate the role of PCs in the ISC competition we modulated PC number (Farin et al., 2012; Yin et al., 2013). While an increase in the number of both ISCs and PCs lead to a stronger ISC competition, an increase in the number of ISCs with a decrease in the number of PCs, did not affect the ISC competition.

We observed that old CR mice had lower ISC competition than old AL mice. This phenotype was completely the opposite of the observed in young mice. In both old and young mice, we observed an increased number and proliferation of the ISCs following CR treatment, while the major observed difference was the different PCs response to CR, pointing once again the PCs as putative drivers of the observed differences in the ISC competition.

The reason why the number of PCs varies between young (increase) and old (decrease) mice in response to CR is not clear. Our hypothesis is that old AL mice have a higher number of PCs with respect to the young AL mice because they are characterized by an increase in pro-inflammatory bacteria, so more PCs may be needed to produce more antimicrobial compounds such as lysozyme and defensins (Zhang et al., 2013; Rasa et al., 2022). Upon CR in old mice the inflammation is reduced (Rasa et al., 2022) as well as pro-inflammatory bacteria decrease together with an increase of anti-inflammatory bacteria (Zhang et al., 2013). Therefore, CR in old mice could change the ISC differentiation far away from the PC lineage.

4. Methods

4.1. Mice

All mice used were on a C57BL6/J background. Double heterozygous Tg(Vil1-cre/ERT2)23Syr;Gt(ROSA)26Sor$^{tm1(CAG-Brainbow2.1)Cle}$ mice (referred in the text as Rosa26-lsl-Confetti;Villin-creERT^2 mice) used for the experiments were derived from breeding of homozygous Rosa26-lsl-Confetti with heterozygous Villin-creERT^2.

Heterozygous Lgr5$^{tm1(cre/ERT2)Cle}$ mice (referred in text as Lgr5-EGFP-IRES-creERT^2 mice) were obtained from breeding Lgr5-EGFP-IRES-creERT^{2}mice with wild-type (WT) (C57BL/6Rj) mice.

Homozygous Olfm4$^{tm2.1(EGFP/cre/ERT2)Cle}$ mice (referred in text as Olfm4-EGFP-IRES-creERT^2 mice) were obtained from breeding of 2 homozygous Olfm4-EGFP-IRES-creERT^2 mice.

All mates were performed at FLI institute and the derived mice were kept in specific pathogen-free animal facilities in FLI institute. All animals were kept in a specific pathogen-free animal facility with a 12 h light/dark cycle. Calorie restriction experiments were performed on female mice. Calorie restriction in young mice was started at the age of 8–14 weeks. In old mice calorie restriction was started at the age of

80–85 weeks.

For the experiments we followed the rules of the state government of Thuringia (Thueringer Landesamt für Verbraucherschutz (TLV)), application licenses (FLI-18–016, O_FN_18–20 and FLI-18–005).

4.2. Calorie restriction

Mice were co-housed in groups of 3–4 animals per cage. The mice were on CR feeding for 39 days. The daily food intake, corresponding to the 70% of food intake of the *ad libitum* animals (AL), was calculated for young mice as: body weight multiplied by the factor 0.13; for old mice as: body weight multiplied by the factor 0.09. A cross-shape divider put inside the cage was used to separate the animals during the feeding. During the morning, each cage was divided into a 4-section cage and each mouse received its own food (ssniff #V1524–786) and jelly water. After 5–6 h the cage divider was removed and the animals regrouped. The AL animals had unlimited access to food and water during the experiment.

4.3. Crypt isolation and organoid culturing

After euthanizing the mouse, the small intestine was dissected and flushed with cold PBS.

The intestine was cut longitudinally and using a glass microscope slide the villi were scraped off. Next, the intestine was cut into small pieces of 2–3 cm and transferred to a 50 ml plastic falcon tube containing 30 ml of ice-cold PBS. After shaking, the pieces were transferred to clean 50 ml plastic falcon tubes containing 30 ml of ice-cold PBS. After shaking, the tissue was transferred to clean 50 ml plastic falcon tubes containing 30 ml of 5 mM EDTA/PBS and placed at 4 ºC for 30 min on rotation shaker for digestion. This last step was repeated twice. The supernatant fraction enriched in crypts was collected, passed through a 70 μm cell strainer and centrifuged for 5 min at 450 rcf at 4ºC. The crypts were then pelleted and resuspended in 1 ml ice-cold PBS. Crypts were embedded with matrigel. The crypts in matrigel were seeded in 24-well plates. Briefly, a total of roughly 250–500 crypts were mixed with 30 μl of matrigel and plated in 24-well plates. After gelling of the matrigel for 5 min at 37 °C, 500 μl of crypt culture medium (Advanced DMEM/F12, B27 and N2 supplement, 50 ng ml^{-1} epidermal growth factor, 100 ng ml^{-1} Noggin, 500 ng ml^{-1} R-spondin-1) was added. CHIR99021 5 μM, CHIR99021 3 μM and Valproic Acid 1 mM, when indicated, were added to the culture.

4.4. 4-Hydroxy-Tamoxifen crypts and organoids treatment

Freshly isolated crypts or already established organoids from Rosa26-lsl-Confetti;Villin-creERT^2 were treated with (Z)− 4-Hydroxytamoxifen ≥ 98% (4-OHT) at a concentration of 5 μM for 20 h. After that 4-OHT conditioned media was substituted with standard crypt culture medium. CHIR99021 5 μM, CHIR99021 3 μM and Valproic Acid 1 mM, when indicated, were added to the culture. The choice of following the organoids for 12/13 days was due to the fact that this was the maximum time that we were able to culture the organoids without passaging.

4.5. Single cell and doublets isolation

After standard crypts isolation (described above) we proceeded to single cell isolation. Single cells were obtained by incubating crypts in complete TrypLE media ($CaCl_2$ 5 μM, $MgCl_2$ 2,5 μM, Tris-HCl 10 μM pH 7.5 and DNAase I 1 mg/ml) for 30 min in a water-bath at 37 °C, pipetting every 10 min with a p1000 to mechanically break-up the cells. Dissociated cells were subsequently passed through cell strainers of 70 and a 40-μm and collected in FACS sorting media (2% FBS, EDTA 3 mM in PBS). Single intestinal stem cells were sorted as Lgr5-GFP high, medium and low cells. Paneth cells were isolated as GFP^{negative}CD24^{high}SideScatter^{high}. Doublets were sorted as Lgr5-GFP$^+$/CD24^{hi}. Dead cells were excluded from the analysis with the viability dye 4′, 6-diamidino-2-phenylindole (DAPI). Isolated single cells were embedded in 10–15 μl matrigel into a U-shape bottom 96-well plate and allowed to solidify for 20–30 min in a 37 °C incubator. After that 150 μl of crypt culture medium (Advanced DMEM/F12, B27 and N2 supplement, 50 ng ml^{-1} epidermal growth factor, 100 ng ml^{-1} Noggin, 500 ng ml^{-1} R-spondin-1) was added. The media was changed every 2 days. 1 mM Jagged-1, when indicated, was added to culture.

4.6. Organoids flow cytometry analysis

Cell culture medium was removed and organoids were dissociated by pipetting 20 times with a p1000 with ice-cold PBS. Organoids were then collected in a 1.5 ml tube and centrifuged at 450 rcf at 4 °C. PBS supernatant was aspirated without disturbing the organoid pellet. Complete TrypLE media was added to the organoids for 20 min in a water bath at 37 °C, pipetting every 10 min with a p1000 to mechanically break-up the cells. Dissociated cells were passed subsequently through cell strainers respectively of 70 and 40 μm and collected in FACS sorting media. The cells were then stained with DAPI and analyzed using a flow cytometer (FACS Canto, BD). For comparisons of GFP expression, DAPI-negative cells were gated as GFP+ and GFP− populations and analyzed using BD FACS Diva software.

4.7. Whole mount preparation

To prepare intestinal whole mounts, the proximal small intestine of Rosa26-lsl-Confetti;Villin-creERT^2 mice were harvested and flushed with ice cold PBS. After fixing the tissue overnight at 4 °C in 4% paraformaldehyde (PFA), the tissue was washed in PBS (3 ×5 min) and then opened longitudinally. Using a cover glass, the villi were scraped off and the tissue was washed in ice cold PBS. After this the tissue was directly mounted between two coverslips using DePeX (Serva 18243.01) for imaging.

4.8. Immunofluorescence staining of paraffin sections

5 μm paraffin sections were deparaffinized by 2 times immersion in xylene (10 min each time) and rehydrated by immersion in a series of graded ethanol dilutions 100%, 90% and 70% for 1 min each. Antigen retrieval was performed using pressure cooker pretreatment in 10 mM sodium citrate buffer pH 6, leaving the samples for 20 min at 95 °C. After cooling down for 30 min, the sections were washed 3 times for 5 min in PBST (Tween 20 0.05% in PBS) and blocked with 5% donkey serum 1% BSA in PBS for 1 h at RT in humid chamber. Sections were then stained, separately, with the following primary antibodies: anti Ki67 rabbit monoclonal (1:100 Abcam, ab-16667), H3-pS10 rabbit (1:200 Upstate 06–570) and anti-GFP-488 goat polyclonal IgG (1:400 Rockland Immunochemicals 600–141–215). All the antibodies used were resuspended in 5% donkey serum 1% BSA in PBS over night at 4 °C in humid chamber. This was followed by washing in PBST (3 ×5 min) and subsequent incubation for 60 min at RT with secondary anti-rabbit AF-568, secondary anti-rabbit AF-647 and secondary anti-goat AF-488 (secondary antibodies dilution 1:500). The slides were washed in PBST (3 ×5 min) and mounted with glass coverslips using mounting medium including DAPI. The slides were stored at + 4 C till further use, and then analyzed using Zeiss ApoTome microscopes.

4.9. Immunohistochemistry staining of paraffin sections

5 μm paraffin sections were deparaffinized by 2 times immersion in xylene (10 min each time) and rehydrated by immersion in a series of graded ethanol dilutions 100%, 90% and 70% for 1 min each. Antigen retrieval was performed using pressure cooker pretreatment in 10 mM sodium citrate buffer pH 6, leaving the samples for 20 min at 95 °C.

After cooling for 30 min, the sections were washed 3 times for 5 min in PBST (Tween 20 0.05% in PBS). For enzymatic detection with HRP-labeled secondary antibody, the endogenous peroxidases were inactivated in 3% H_2O_2 in H_2O. After washing (3 ×5 min), the sections were incubated with blocking solution (5% donkey serum 1% BSA in PBS) for 1 h at RT in a humid chamber. Subsequently, the sections were washed with PBST (3 ×5 min) and incubated with the primary antibody: Olfm4 (D6Y5A) rabbit monoclonal antibody (1:200 Cell Signaling 39141) overnight at 4 °C in a humid chamber. Next day the sections were washed with PBST (3 ×5 min). For the enzymatic detection of proteins, a biotinylated secondary antibody (donkey anti-rabbit) was diluted 1:100 in PBS and incubated for 45 min at RT in humid chamber. The sections were washed with PBST (3 ×5 min). For enzymatic staining the avidin-biotin complex (ABC) solution (Vector Labs) was prepared 20 min before use by 1 drop of solution A and one drop of solution B in 5 ml PBS and well mixed. The sections were then incubated for 1 h with the ABC complex at RT in a humid chamber and washed in PBST (3 ×5 min). Development was carried out with DAB chromogen. The enzymatic reaction was stopped in distilled water when sufficiently brown in color. For better contrast, the sections were counterstained with hematoxylin and mounted with glass coverslips and aqueous mounting medium (Aquatex, Merck, #1085620050). The slides were stored at + 4 C till further use, and then evaluated using Leica and Zeiss Microscopes.

4.10. Immunofluorescence staining of cryo-sections

Antigen retrieval was performed using pressure cooker pretreatment in 10 mM sodium citrate buffer pH 6, leaving the samples for 20 min at 95 °C. After cooling for 30 min, the sections were washed 3 times for 5 min in PBST (Tween 20 0.05% in PBS) and blocked with 5% donkey serum, 1% BSA in PBS for 1 h at RT in a humid chamber. Sections were then stained with the following primary antibodies: anti-human lysozyme EC 3.2.1.17 rabbit polyclonal (1:250) Dako Agilent A0099 (02−2)) and Lysozyme C (H-10) mouse monoclonal (1:200 Santa Cruz sc-518083). All the antibodies used were resuspended in 5% donkey serum, 1% BSA in PBS over night at 4 °C in a humid chamber. This was followed by washing in PBST (3 ×5 min) and subsequent incubation for 60 min at RT with secondary anti-rabbit AF-568, secondary anti-rabbit AF-647 and secondary anti-goat AF-488 (secondary antibodies dilution 1:500). The slides were washed in PBST (3 ×5 min) and mounted with glass coverslips using a mounting medium including DAPI. The slides were stored at + 4 C till further use, and then analyzed using Zeiss ApoTome microscopes.

4.11. Whole mount staining of intestinal organoids

The crypts were embedded with Matrigel and seeded on 8 well glass slides (Thermo Fisher 16260661). After gelling of the Matrigel for 5 min at 37 °C, 300 µl of crypt culture medium (Advanced DMEM/F12, B27 and N2 supplement, 50 ng µl−1 epidermal growth factor, 100 ng ml−1 Noggin, 500 ng µl−1 R-spondin-1) was added. CHIR99021 5 µM, CHIR99021 3 µM and Valproic Acid 1 mM, when indicated, were added to the culture. At the moment of staining media was removed and this was followed by a washing (1 ×5 min) with PBS). Organoids were then fixed with 4% paraformaldehyde (PFA) for at least 30 min at RT. This was followed by washing in PBS (3 ×5 min) and subsequent permeabilization step with 0.5% Triton in PBS for 30 min at RT. The organoids were then washed in PBS (3 ×5 min). Blocking was performed with 5% donkey serum, 0.25% Triton X 100 in PBS for 30 min at RT in a humid chamber. Sections were then stained with the following primary antibodies: anti-human lysozyme EC 3.2.1.17 rabbit polyclonal (1:250) Dako Agilent A0099 (02−2) and anti-GFP-488 goat polyclonal IgG (1:400) Rockland Immunochemicals 600–141–215). All the antibodies used were resuspended in blocking buffer over night at 4 °C in a humid chamber. The next day the organoids were washed with PBS (3 ×5 min) and this was followed by subsequent overnight incubation at 4 °C in a humid chamber with secondary anti-rabbit AF-568 and secondary anti-goat AF-488 (secondary antibodies dilution 1:500). Next day organoids were washed in PBS (3 ×5 min). They were stained with DAPI for 30 min at RT, followed by a washed with PBS (1 ×5 min). The slides were stored at + 4 C till further use, and then analyzed using Zeiss ApoTome microscope (for live imaging).

4.12. Statistical analysis

Statistical analysis was made using GraphPad Prism software 7.0c. Unpaired two-tails t-test, unpaired two-tails t-test with Welch's correction and Mann-Whitney test were used to calculate the significance: a pValue < 0.05 was considered significant. Shapiro Wilk test was used to calculate the normality before to apply the test. Mann-Whitney test was applied only in the cases where there was not normal distribution of the values. Unpaired two-tails t-test with Welch's correction was used in case populations had different Standard Deviations (SD).

CRediT authorship contribution statement

Francesco Annunziata: Conceptualization, Project administration, Investigation, Methodology, Data curation, Validation, Visualization, Writing – original draft preparation. **Seyed Mohammad Mahdi Rasa:** Methodology, Visualization, Writing – review & editing. **Anna Krepelova:** Supervision, Visualization, Writing – review & editing. **Jing Lu**: Visualization, Writing – review & editing. **Alberto Minetti**: Visualization, Writing – review & editing. **Omid Omrani**: Visualization, Writing – review & editing. **Suneetha Nunna**: Visualization, Writing – review & editing. **Lisa Adam**: Methodology. **Sandra Käppel**: Methodology. **Francesco Neri**: Funding acquisition, Conceptualization, Project administration, Investigation, Data curation, Visualization, Writing – original draft.

Declaration of Competing Interest

The authors declare that they have no known competing financial interests or personal relationships that could have appeared to influence the work reported in this paper.

Acknowledgments

We would like to thank our colleagues from the Fritz Lipmann Institute Core Facilities and Services: Flow Cytometry, DNA Sequencing, Imaging, and Animal Facilities for their assistance throughout the course of this study. This work was supported by funding from Alexander von Humboldt foundation (1164767-ITA-SKP) and the Leibniz Institute on Aging (FLI).

Appendix A. Supporting information

Supplementary data associated with this article can be found in the online version at doi:10.1016/j.ejcb.2022.151282.

References

Azkanaz, M., et al., 2022. Retrograde movements determine effective stem cell numbers in the intestine. Nature 607, 548–554. https://doi.org/10.1038/s41586-022-04962-0.

Barker, N., et al., 2009. Crypt stem cells as the cells-of-origin of intestinal cancer. Nature 457 (608), 612. https://doi.org/10.1038/nature07602.

Bruens, L., et al., 2020. Calorie restriction increases the number of competing stem cells and decreases mutation retention in the intestine. CellReports 32 (3), 107937. https://doi.org/10.1016/j.celrep.2020.107937.

Colman, R.J., et al., 2009. Caloric restriction delays disease onset and mortality in rhesus monkeys. Science 325 (5937), 201–204. https://doi.org/10.1126/science.1173635.

Cui, H., et al., 2019. Wnt signaling mediates the aging-induced differentiation impairment of intestinal stem cells. Stem Cell Rev. Rep. 449 (54), 1003–1008. https://doi.org/10.1007/s12015-019-09880-9.

Farin, H.F., van Es, J.H., Clevers, H., 2012. Redundant sources of wnt regulate intestinal stem cells and promote formation of paneth cells, 1518–1529.e7 *YGAST* 143. https://doi.org/10.1053/j.gastro.2012.08.031.

Fontana, L., Partridge, L., Longo, V.D., 2010. Extending healthy life span–from yeast to humans. Science 328 (5976), 321–326. https://doi.org/10.1126/science.1172539.

Huels, D.J., et al., 2018. Wnt ligands influence tumour initiation by controlling the number of intestinal stem cells, 1132–10 Nat. Commun. 9 (1). https://doi.org/10.1038/s41467-018-03426-2.

Igarashi, M., Guarente, L., 2016. mTORC1 and SIRT1 cooperate to foster expansion of gut adult stem cells during calorie restriction. Cell 1–16. https://doi.org/10.1016/j.cell.2016.05.044.

Janeckova, L., et al., 2016. Wnt signaling inhibition deprives small intestinal stem cells of clonogenic capacity. Genesis 54 (3), 101–114. https://doi.org/10.1002/dvg.22922.

Kabiri, Z., et al., 2018. Wnt signaling suppresses MAPK-driven proliferation of intestinal stem cells. J. Clin. Investig. 128 (9), 3806–3812. https://doi.org/10.1172/JCI99325.

Lopez-Garcia, C., 2010. Intestinal stem cell replacement follows a pattern of neutral drift. Science 330 (6005), 822–825. https://doi.org/10.1126/science.1196236.

Mihaylova, M.M., et al., 2018. Fasting activates fatty acid oxidation to enhance intestinal stem cell function during homeostasis and aging. Stem Cell 22, 769–778.e4. https://doi.org/10.1016/j.stem.2018.04.001.

Nalapareddy, K., et al., 2017. Canonical Wnt signaling ameliorates aging of intestinal stem cells. CellReports 18, 2608–2621. https://doi.org/10.1016/j.celrep.2017.02.056.

Oh, J., Lee, Y.D., Wagers, A.J., 2014. Stem cell aging: mechanisms, regulators and therapeutic opportunities. Nat. Med. 20 (8), 870–880. https://doi.org/10.1038/nm.3651.

Pentinmikko, N., et al., 2019. Notum produced by Paneth cells attenuates regeneration of aged intestinal epithelium. Nature 571 (7765), 398–402. https://doi.org/10.1038/s41586-019-1383-0.

Rasa, et al., 2022. Inflammaging is driven by upregulation of innate immune receptors and systemic interferon signaling and is ameliorated by dietary restriction. CellReports 39, 111017. https://doi.org/10.1016/j.celrep.2022.111017.

Sato, T., et al., 2009. Single Lgr5 stem cells build crypt-villus structures in vitro without a mesenchymal niche. Nature 459 (7244), 262–265. https://doi.org/10.1038/nature07935.

Sato, T., et al., 2010. Paneth cells constitute the niche for Lgr5 stem cells in intestinal crypts. Nature 469 (7330), 415–418. https://doi.org/10.1038/nature09637.

Snippert, H.J., et al., 2010. Intestinal crypt homeostasis results from neutral competition between symmetrically dividing Lgr5 stem cells. Cell 143 (1), 134–144. https://doi.org/10.1016/j.cell.2010.09.016.

Uchida, R., Saito, Y., et al., 2019. Epigenetic silencing of Lgr5 induces senescence of intestinal epithelial organoids during the process of aging. Npj Aging Mech. Dis. 1–9. https://doi.org/10.1038/s41514-018-0031-5.

van der Flier, L.G., Clevers, H., 2009. Stem cells, self-renewal, and differentiation in the intestinal epithelium. Annu. Rev. Physiol. 71 (1), 241–260. https://doi.org/10.1146/annurev.physiol.010908.163145.

Vermeulen, L., et al., 2013. Defining stem cell dynamics in models of intestinal tumor initiation. Science 342, 995–998. https://doi.org/10.1126/science.1243148.

Winton, D.J.and Ponder, B.A. Stem-cell organization in mouse small intestine. Proceedings. Biological Sciences, 241(1300), 13–18. http://doi.org/10.1098/rspb.1990.0059 (1990).

Yilmaz, O.H., et al., 2012. mTORC1 in the Paneth cell niche couples intestinal stem-cell function to calorie intake. Nature 486 (7404), 490–495. https://doi.org/10.1038/nature11163.

Yin, X., et al., 2013. Niche-independent high-purity cultures of Lgr5+ intestinal stem cells and their progeny. Nat. Methods 11, 106–112. https://doi.org/10.1038/nmeth.2737.

Zhang, C., et al., 2013. Structural modulation of gut microbiota in life-long calorie restricted mice. Nat. Commun. 4, 2163. https://doi.org/10.1038/ncomms3163.